

A Broad-Band Microwave Circulator*

EDWARD A. OHM†

Summary—The discovery of a simple, low loss way to hold Faraday rotation constant over a broad-band (coupled with the development of wide-band, high return loss, circular-to-rectangular waveguide transformers, and polarization couplers) has made it possible to design and build a high quality circulator for use in the 10.7 kmc to 11.7 kmc band.

The essential characteristics of the described unit include a more than 30-db return loss at each terminal, an isolation of 30 db or greater between "isolated" terminals, and a 0.35-db insertion loss between transmission terminals.

I. INTRODUCTION

THE PRINCIPLES of a four-arm Faraday rotation circulator were first published by Hogan in 1952.¹ Now with the discovery of a simple, low-loss way to hold Faraday rotation constant with frequency, it has been possible to design a good, practical circulator for use over at least a 10 per cent band.

The ideas and techniques which are discussed here can be applied to any waveguide frequency band. However, since there was a special interest in the 10.7-kmc to 11.7-kmc band, this data will be used for illustration.

The objective, of course, is to design an ideal circulator, and an ideal Faraday rotation circulator is shown in Fig. 1. Energy entering in arm 1 is polarized in the

If the waveguide plumbing is nearly lossless and its reflections are small compared to those of the ferrite loaded region then all of the circulator characteristics will be determined by the ferrite-loaded region itself. This is a situation which can be approximated in practice and the necessary techniques for designing the waveguide components are described in part III.

In the design of a broad-band Faraday rotation circulator there are then three main things which degrade the performance from that of an ideal circulator.

1) The insertion loss of the ferrite assembly (*i.e.*, all of the materials which are inserted in the ferrite loaded region). This, of course, causes transmission loss between the transmission arms of the circulator.

2) A change of Faraday rotation with frequency. This causes adjacent arm leakages between nontransmission terminals as shown by the dashed lines in Fig. 3. For example (refer to Fig. 1), if energy entering arm 1 polarized as E_1 is not rotated exactly 45° , then its polarization will not be completely in the plane of E_2 but will have a component in the E_4 direction and this component will pass directly into arm 4. The isolation of this type of leakage can be computed and it is:

$$\text{Isolation} = 20 \log_{10} \csc \Delta\theta^\circ \text{ db} \quad (1)$$

where $\Delta\theta^\circ$ is the departure in rotation from 45° .

3) Reflection from the ferrite assembly. This determines the return loss of each circulator arm and what is more important it causes alternate arm leakages as shown by the dashed lines in Fig. 4. For example (refer to Fig. 1), if energy from arm 1 is partially reflected by the far end of the ferrite assembly this reflected energy will reverse its direction, rotate another 45° to the polarization of arm 3 and pass directly into arm 3. The isolation of this type of leakage is equal to the return loss of the ferrite assembly.

Figs. 5-8 show four typical circulator applications first suggested by A. G. Fox, S. E. Miller, and W. W. Mumford of Bell Telephone Laboratories. The dashed lines indicate leakage paths which would most seriously interfere with the performance of each broad-band system. As seen from these figures both types of leakage are equally troublesome and therefore the design objective for this general purpose circulator was to attain an equal minimum of both types of leakage, commensurate with the smallest possible insertion loss.

The adjacent arm leakage due to a change in Faraday rotation with frequency has been the most serious obstacle in the design of a good broad-band circulator. The next section shows a general solution of this problem as well as a particular solution which more nearly satisfies the arbitrary design objectives.

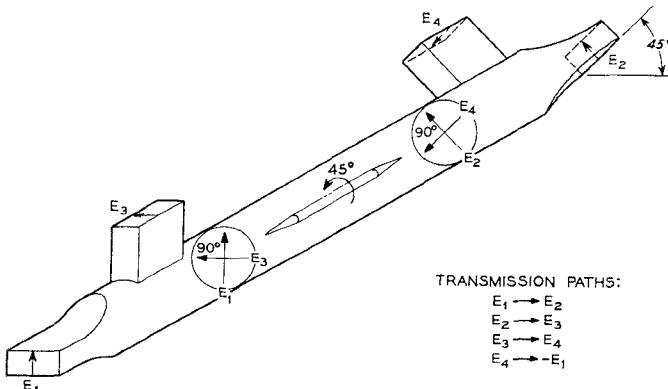


Fig. 1—An ideal circulator.

direction E_1 and on passage through the ferrite loaded region its polarization is rotated exactly 45° to the plane of E_2 . Thus, all of the energy passes exclusively from arm 1 to arm 2. In a like manner energy entering arm 2 passes exclusively to arm 3, energy entering arm 3 passes exclusively to arm 4, and energy entering arm 4 passes exclusively to arm 1. This is shown symbolically in Fig. 2 (opposite).

* Manuscript received by the PGMTT, July 16, 1956. Presented before the National Symposium on Microwave Techniques, Philadelphia, Pa., February 2-3, 1956.

† Bell Telephone Labs., Holmdel, N. J.

¹ C. L. Hogan, "The ferromagnetic Faraday effect at microwave frequencies and its applications," *Bell Sys. Tech. J.*, vol. 31, pp. 1-31; January, 1952. See p. 25.

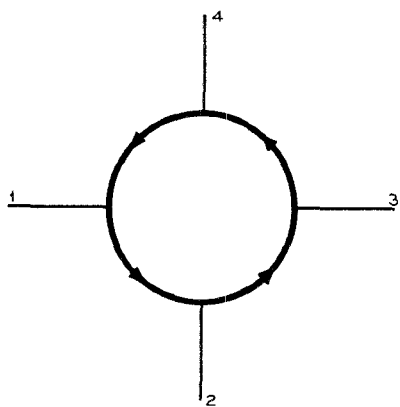


Fig. 2—An ideal circulator symbol.

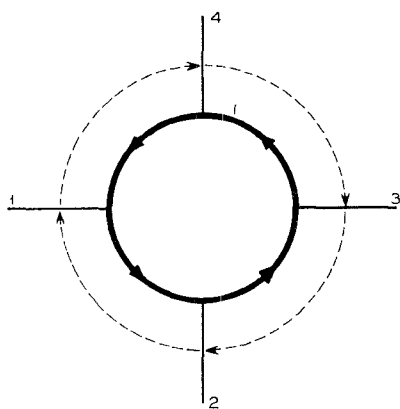
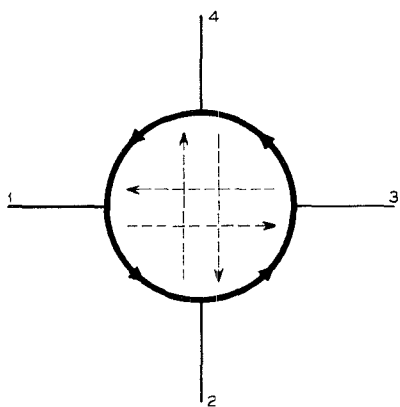
Fig. 3—A circulator with leakage due to a variation, $\Delta\theta$, from 45° rotation.

Fig. 4—A circulator with leakage due to ferrite assembly return loss.

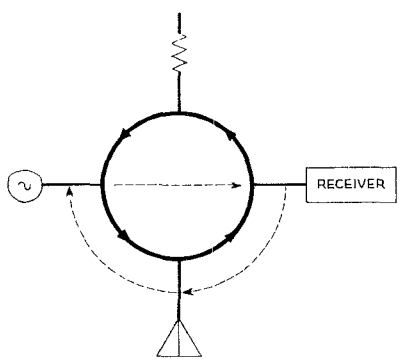


Fig. 5—A circulator duplexer.

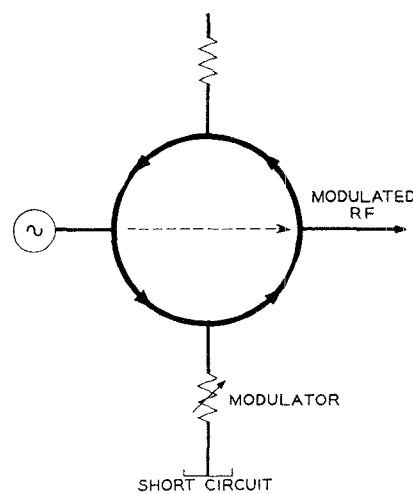


Fig. 6—A circulator microwave modulator.

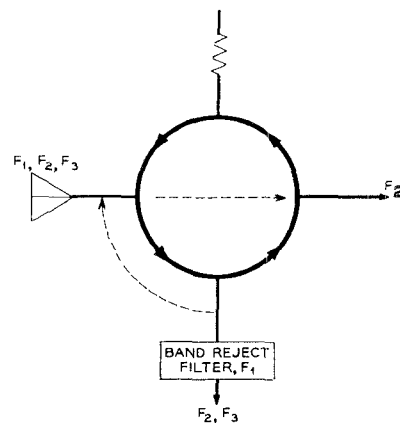


Fig. 7—A circulator channel brancher.

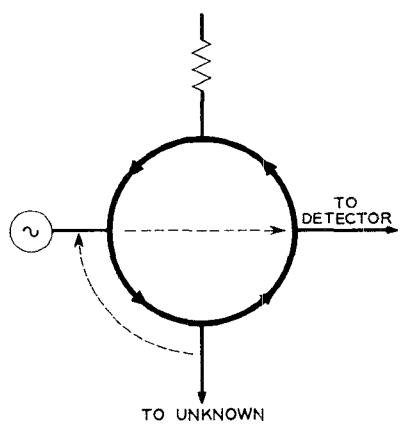


Fig. 8—A circulator as a no-loss directional coupler and isolator.

II. BROADBANDING FARADAY ROTATION

The Faraday rotation of a ferrite cylinder (with conical matching tapers) centered in round waveguide increases considerably with frequency as shown by the upper curve of Fig. 9. Since a theoretical infinite medium of ferrite does not predict this frequency dependence it has been suggested that this is due to an increase in the percentage of energy in the ferrite (as the fre-

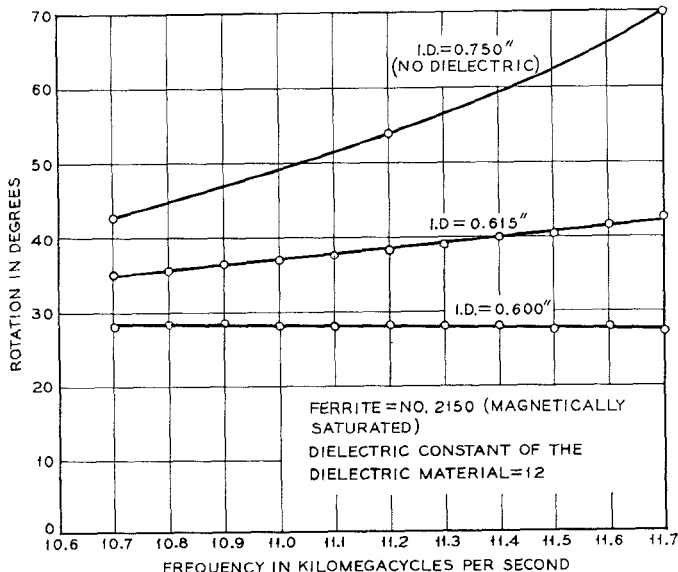
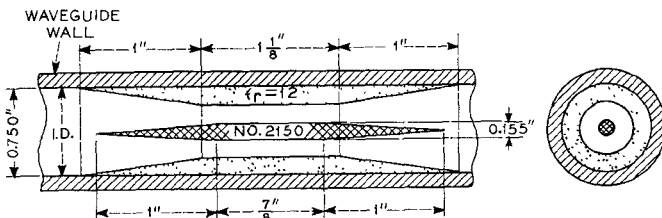


Fig. 9—Variation of rotation as a function of frequency and dielectric inside diameter ($\epsilon_r=12$).

quency is increased) in a manner analogous to the dielectric waveguide effect.² If this is true, it seemed that a hollow concentric tube (with conical matching tapers) of high dielectric constant material could be inserted with its outside diameter contiguous to the waveguide wall and this would produce in the central region a compensating dielectric waveguide effect. Both of these ideas were confirmed by the curves of Fig. 9. As the dielectric material inside diameter was decreased (*ie.*, indicates an increase in the amount of dielectric material) the Faraday rotation decreased, the slope decreased, and it was even possible to obtain a negative slope in this manner. The lower curve of Fig. 9 shows a rotation characteristic of zero slope which is completely independent of frequency in this band.

The insertion loss of this latter ferrite assembly for 45° rotation was approximately 0.65 db and the major part of this loss was due directly to the loss tangent of the relatively high dielectric constant material ($\epsilon_r=12$). Since lower dielectric constant materials generally have a lower loss tangent an effort was made to discover whether or not this phenomenon would be effective using lower dielectric constant materials. Some of these results using polystyrene ($\epsilon_r=2.55$) and the same ferrite

² G. C. Southworth, "Principles and Applications of Wave Guide Transmission," D. Van Nostrand Co., Inc., p. 129; 1954.

cylinder are shown in the top locus of Fig. 10. As the dielectric material inside diameter was decreased, the rotation ratio³ decreased to a minimum before it again began to increase. By using smaller diameter cylinders of the same ferrite material the rotation ratio could even be reduced to less than unity and this is illustrated by the lowest locus of Fig. 10.

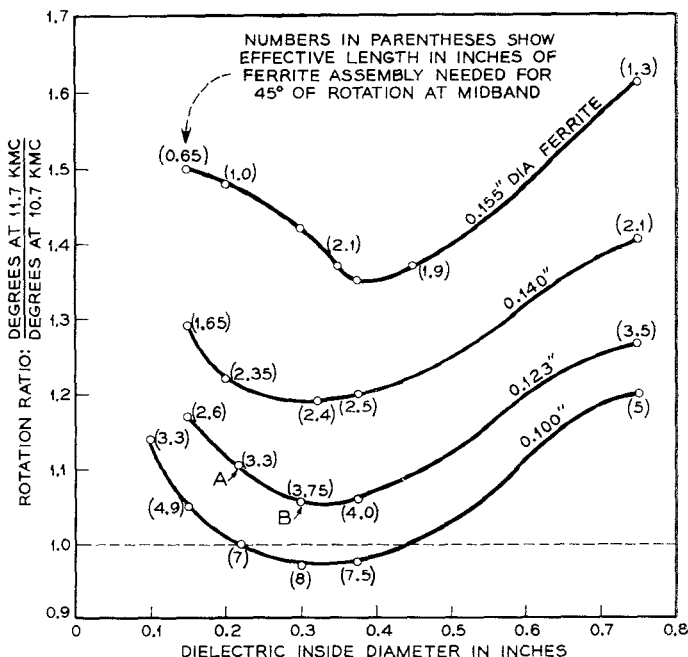


Fig. 10—Variation of rotation ratio for different ferrite diameters using $\epsilon_r=2.55$ material in 0.750-inch diameter waveguide.

The insertion losses of ferrite assemblies using polystyrene were less than other materials tested (for similar rotations and rotation ratios) and most of the total losses were caused by either the loss tangent of the polystyrene or an increase in copper loss due to the polystyrene presence. Whatever the exact cause, losses were roughly proportional to the quantity of polystyrene especially for the smaller diameter ferrite samples. Since the optimum polystyrene inside diameter is nearly constant for the ferrite diameters of interest (see Fig. 10) it was concluded that the quantity of polystyrene and thus loss is roughly proportional to the ferrite assembly effective length.

³ Since the rotation of each ferrite assembly under discussion here changes nearly linearly with frequency (as typified by the $id=0.615$ -inch locus of Fig. 9) the rotation ratio is a convenient index of the rotation vs frequency slope and can be easily used to predict $\Delta\theta$.

$$\Delta\theta = \frac{\theta_2/\theta_1 - 1}{\theta_2/\theta_1 + 1} \theta_0 \quad (2)$$

where

θ_2/θ_1 = rotation ratio,

θ_2 = rotation at highest frequency in band,

θ_1 = rotation at lowest frequency in band,

θ_0 = desired rotation at midband (usually 45°),

$\Delta\theta$ = rotation departure from midband rotation.

The length of ferrite assembly required for 45° of rotation at midband increased as the minimums in rotation ratio approached the optimum goal of unity and these effective lengths in inches are shown in parenthesis in Fig. 10. Therefore, since the ferrite assembly losses are proportional to the effective length, a unity rotation ratio would also lead to a larger insertion loss.

Diverging for a moment, an investigation of the reflections of this type of assembly indicated that a minimum return loss of more than 33 db would be extremely difficult to achieve over the 10.7-kmc to 11.7-kmc band, and this of course would be a limiting factor in the alternate arm isolation.

Recalling now the design objective of equal values of alternate arm and adjacent arm isolations, it became apparent that a slightly greater than unity rotation ratio could maintain adjacent arm isolations equal to 33 db at the band edges [as per (1) and (2)] and at the same time reduce the transmission path insertion loss. Therefore, point *B* of Fig. 10 was selected as a good compromise and the ferrite assembly and its characteristics stemming from this point are in Fig. 11.

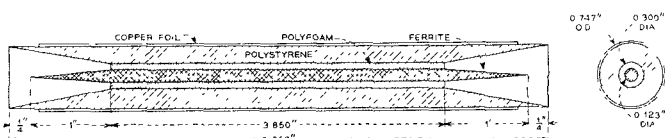


Fig. 11—Circulator ferrite assembly. Ferrite assembly characteristics (ferrite is magnetically saturated).

- 1) Rotation at 11.2 kmc = 45°.
- 2) Rotation ratio, θ at 11.7 kmc / θ at 10.7 kmc = 1.06; therefore, $\Delta\theta = 1.3^\circ$.
- 3) Isolation at band edge (due to E component \perp to the ideal rotation of 45°). Isolation (in db) = $20 \log_{10} \csc \Delta\theta = 33$ db.
- 4) Insertion loss = 0.19 db.
- 5) Return loss ≥ 28 db.

Note that the band edge adjacent arm leakage due to a change in rotation with frequency is 33 db and this is of the same general level as the return loss plotted in Fig. 12. This latter plot would be identical to the alternate arm leakage when the assembly is used in a circulator were it not for the adjusted phasing of smaller reflections from the other circulator components.

The measured insertion loss of this simple ferrite assembly was only 0.19 db and this was considered a reasonable price to pay for the greater than 30 db circulator isolations attainable over the 10.7-kmc to 11.7-kmc band.

III. WAVEGUIDE COMPONENTS

Now that it is apparent that the isolations and return losses of the ferrite assembly can be made greater than 30 db over the 10.7-kmc to 11.7-kmc frequency band it will next be shown how these circulator char-

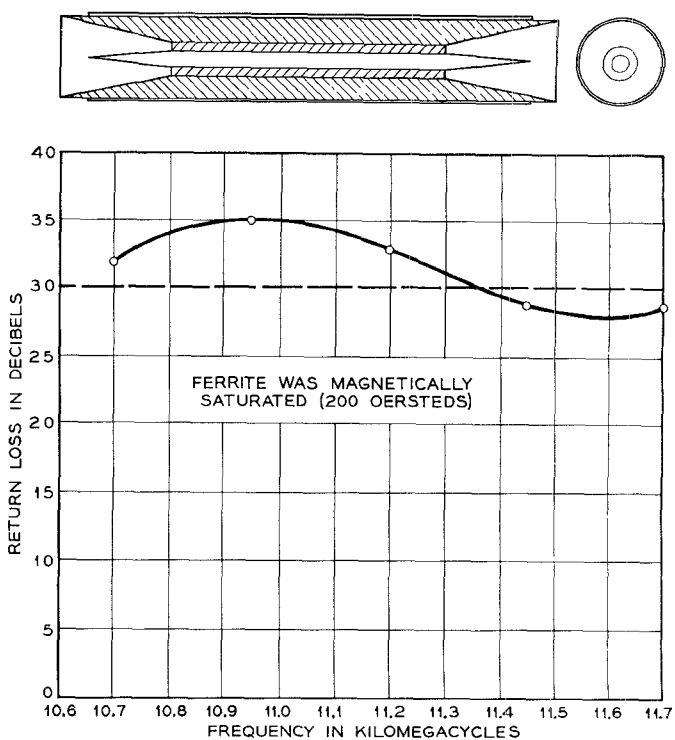


Fig. 12—Return loss of ferrite assembly.

acteristics were preserved by the improved design of wide-band waveguide components.

Short Rectangular-to-Circular Waveguide Transformers

Fig. 13 shows a multiple quarter-wave rectangular-to-circular waveguide transformer designed so that each rectangular-to-rectangular junction has a net zero susceptance at midband. The capacitive shunt susceptance created by a step in waveguide height is cancelled at the same longitudinal location by an inductive shunt susceptance created by a step in waveguide width. Note that these steps are always in opposite directions, *i.e.*, the height of an adjacent section is larger when its width is smaller.

This makes it possible to nonsusceptively couple some waveguides of greatly different aspect ratios and since a standard rectangular waveguide has an aspect ratio of approximately 2 and a circular waveguide has an aspect ratio of 1, this approach automatically breaks up the total metallic discontinuity (of commonly used round and rectangular waveguides) so that it is distributed in a manner which (for a given number of intermediate transformer sections) yields the lowest possible Q at each junction. In this application all of the Q 's were so low that they did not seriously effect the transformer characteristic even at the band edges so all junctions could be treated as pure resistive discontinuities.

Fig. 14 was developed to compute all of the intermediate waveguide transformer dimensions and the procedure is as follows.

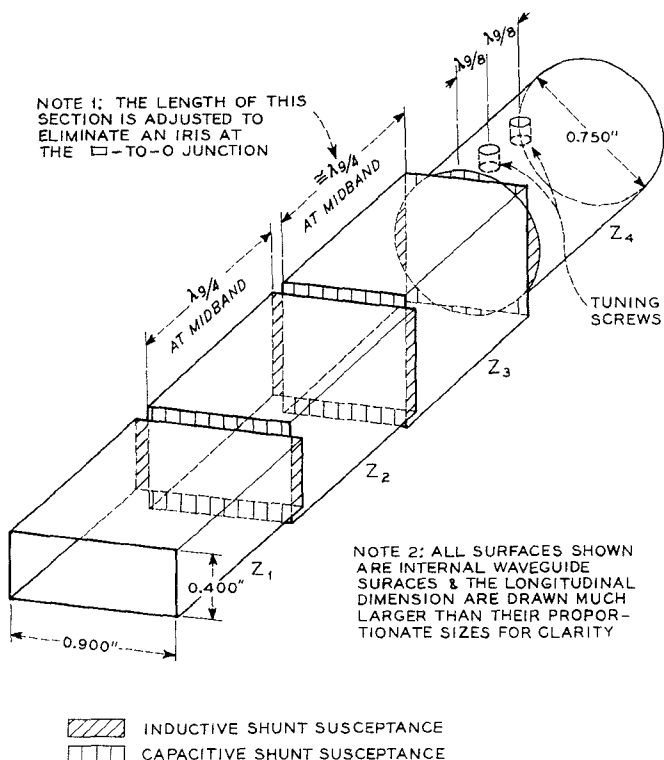


Fig. 13—A multiple quarter-wave transformer with junction susceptance cancellation.

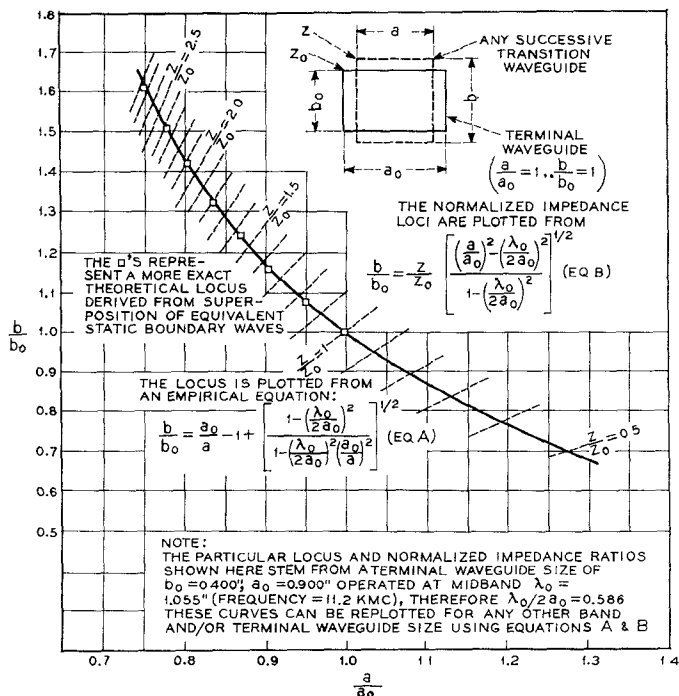


Fig. 14—A locus of waveguide dimension ratios which result in nonsusceptive junction.

- 1) Find the intermediate Z levels using any multiple quarter-wave transformer theory and normalize these to the terminal rectangular waveguide. These are Z/Z_0 .
- 2) Plot these values of Z/Z_0 . From the intersections

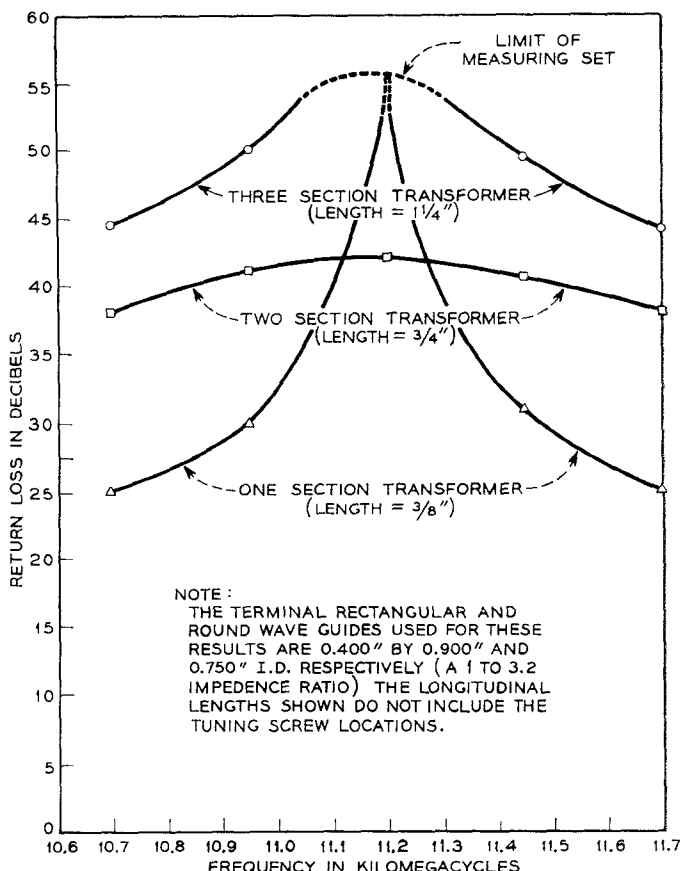


Fig. 15—Experimental results of 1, 2, and 3-section transformers.

of Z/Z_0 with the nonsusceptive locus read the required normalized height b/b_0 , and width a/a_0 , of each transformer section.

3) Denormalize, obtain height, b , and width, a , of each section.

4) Make each section $\lambda_g/4$ long at midband.

This in principle completes the transformer design. It turns out in practice that the arbitrary net susceptance at the rectangular-to-circular junction is fortuitously a small finite value and, in a manner shown by Cohn, a compensating iris at this junction is avoided by slightly altering the length of the waveguide section adjacent to the round waveguide.⁴

The two tuning screws located in the round waveguide were added to correct for a small systematic impedance level error inherent in this type of rectangular-to-rectangular junction and also to act as trimmers to compensate for machining deviations.

All of the over-all results are in excellent agreement with theory and Fig. 15 shows the measured return loss of a one, two, and three section rectangular-to-circular

⁴ S. B. Cohn, "Optimum design of stepped transmission-line transformers," IRE TRANS., vol. MTT-3, pp. 16-21; April, 1955. See p. 18.

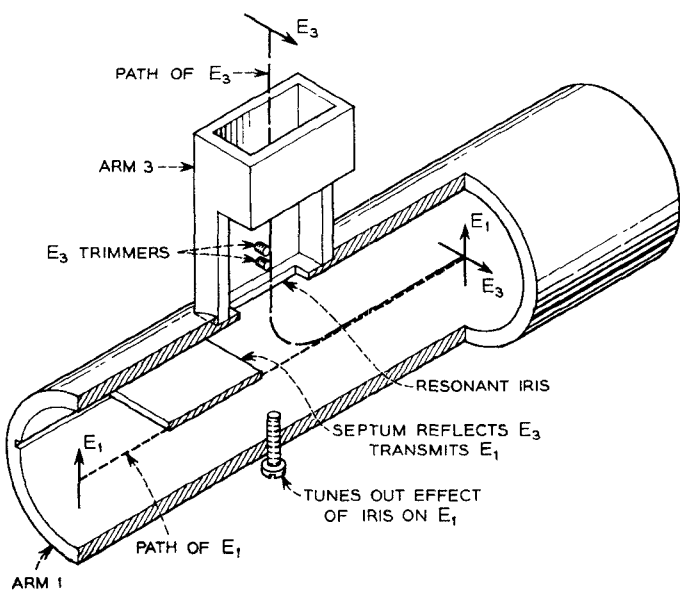


Fig. 16—A mode selecting coupler.

waveguide transformer used to connect the terminal waveguides of Fig. 13 (a 1 to 3.2 impedance ratio). The return loss of the three-section transformer is always greater than 44 db in the 10.7-kmc to 11.7-kmc band and therefore it was chosen for use with this circulator because its over-all reflections are so small that they can hardly interact with the reflections of the other components. In conclusion, note that this transformer is only $1\frac{1}{4}$ inches long (excluding the tuning screw locations) and this short length in itself reduces the copper insertion loss to a negligible value (less than 0.01 db).

A Mode Selecting Coupler

Fig. 16 shows the mechanical details of a mode selecting coupler which evolved at Holmdel of the Bell Telephone Laboratories through contributions by C. F. Edwards, C. B. Feldman, A. P. King, and D. H. Ring. It can be seen that the round waveguide on the right can be used as a mount for the ferrite assembly and by attaching a three-section rectangular-to-circular waveguide transformer to arm 1, the orthogonal polarizations of the round waveguide can be coupled directly and independently to standard rectangular waveguides.

By proper selection of the resonant iris dimensions and careful balancing of the tuning adjustments it was found that the return loss of each arm of the mode selecting coupler assembly could be maintained greater than 35 db over the 10.7-kmc to 11.7-kmc band as shown in Fig. 17, and that the isolation between arms 1 and 3 could be maintained greater than 45 db over this same frequency band. Although the reflections only 35 db down are large enough to degrade the over-all circulator characteristics (by interacting with the ferrite assembly reflections), these effects can be minimized by properly spacing the critical components as disclosed in section IV.

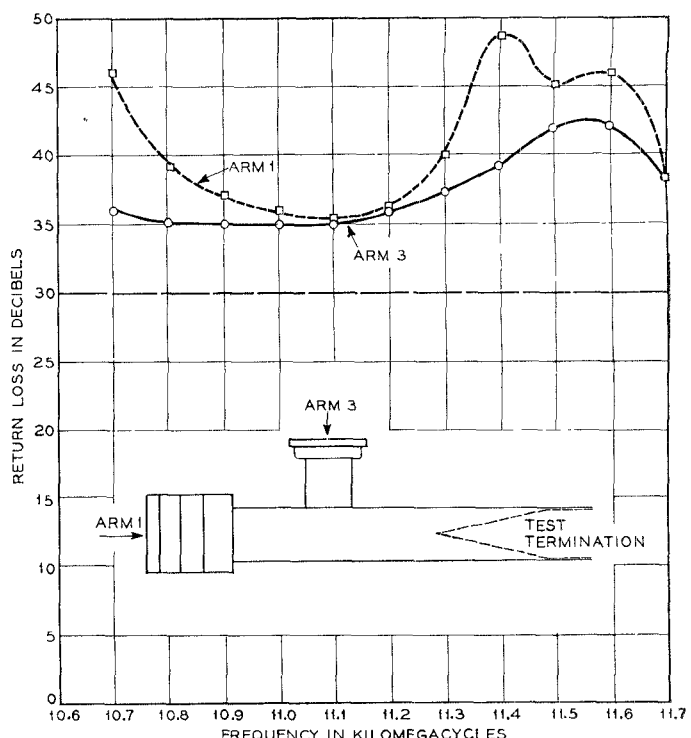


Fig. 17—Return loss of the mode selecting coupler assembly.

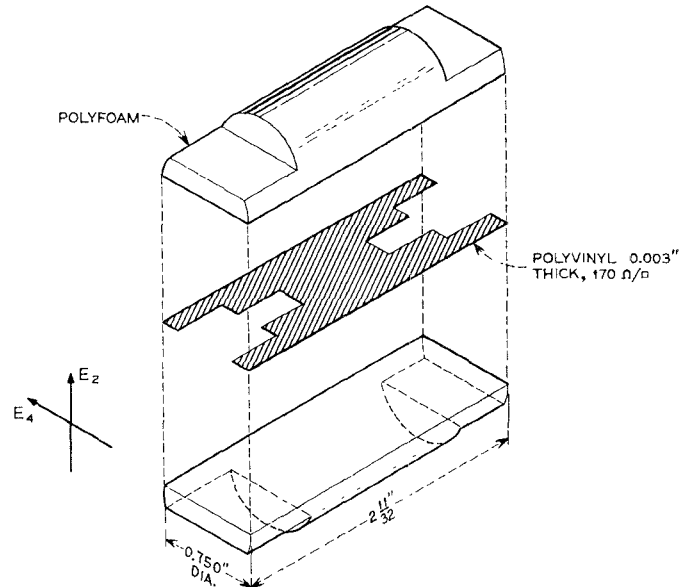


Fig. 18—A mode termination.

- 1) Return loss of $E_2 \geq 45$ db.
- 2) Return loss of $E_4 \geq 40$ db.
- 3) Insertion loss of $E_2 \approx 0$ db.
- 4) Insertion loss of $E_4 \approx 60$ db.

A Mode Selecting Termination

For many circulator applications it is necessary to terminate the 4th arm. Instead of externally terminating an arm of a mode selecting coupler assembly this can be accomplished directly in the round waveguide with negligible effect on the orthogonal polarization by using the mode selecting termination shown in Fig. 18.

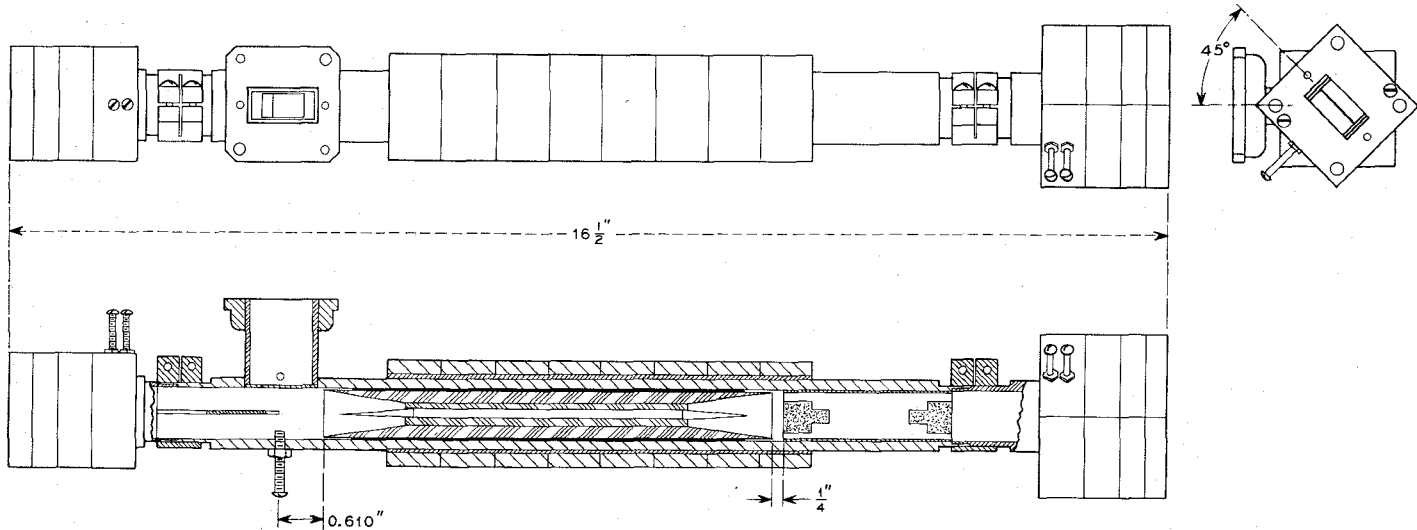


Fig. 19—Microwave circulator assembly.

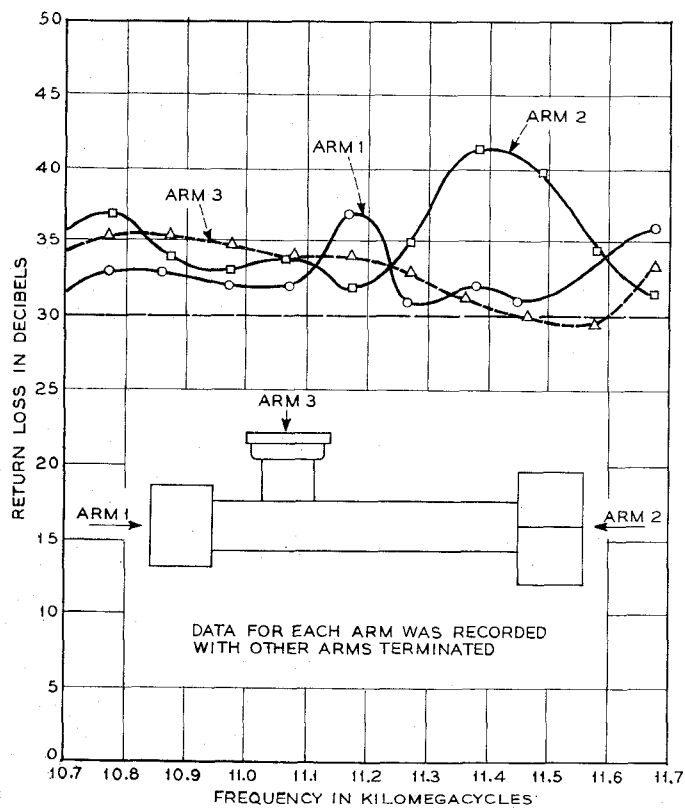


Fig. 20—Circulator return loss.

The return loss of the terminated polarization is more than 40 db and the return loss of the transmitted polarization is more than 45 db over the 10.7-kmc to 11.7-kmc band.

IV. THE CIRCULATOR ASSEMBLY AND EXPERIMENTAL RESULTS

The circulator components were assembled as shown in Fig. 19 and the optimum longitudinal positions of the

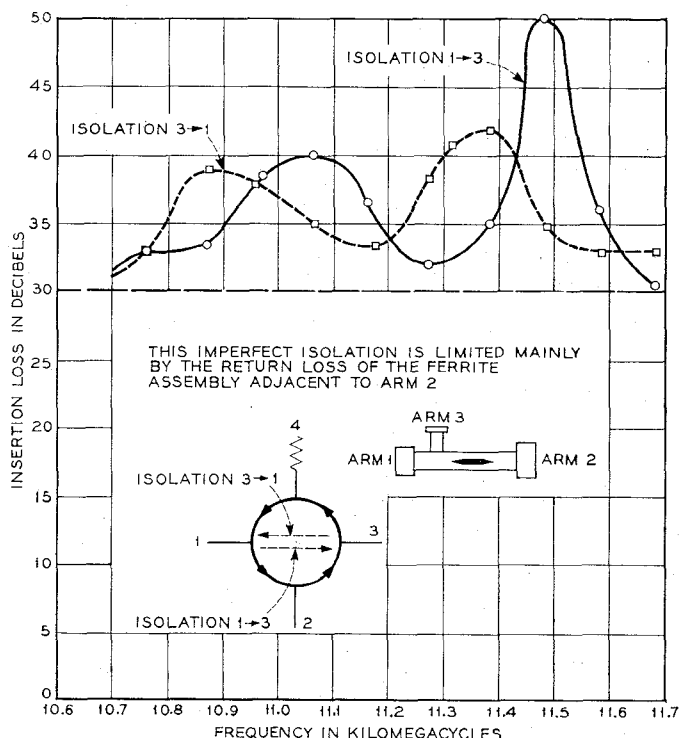


Fig. 21—Circulator isolation of alternate arms.

ferrite assembly and mode selecting termination were determined as follows.

The ferrite assembly was inserted in the mode selecting coupler assembly and after adjusting the magnets for 45° rotation it was located so that the reflections from the adjacent or left end of the ferrite assembly were partially cancelled by those of the mode selecting coupler assembly. Thus the reflections indicated by Figs. 12 and 17 were phased to give the best over-all return loss of arms 1 and 3 as shown in Fig. 20.

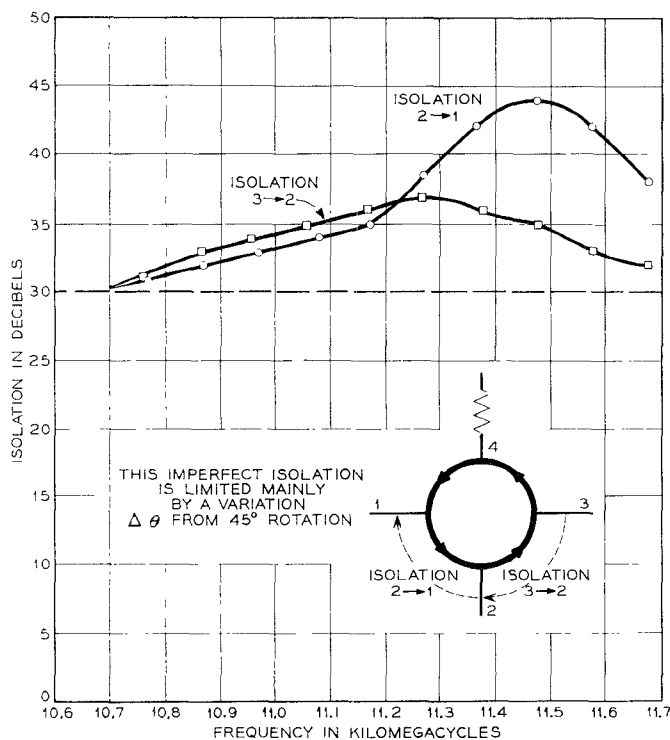


Fig. 22—Circulator isolation of adjacent arms.

The mode selecting termination was then inserted and spaced longitudinally so that both orthogonal reflections from the arm 2 or right end of the ferrite assembly were partially cancelled by the smaller reflections from the mode selecting termination. The resultant reflections determined the alternate arm isolations and these results are shown in Fig. 21. Reflections from these same sources and the arm 2 transformer resulted in the over-all return loss of arm 2 and this data is shown in Fig. 20.

The measured adjacent arm isolations are shown in Fig. 22 and they are about as anticipated. The peaks are not infinite because of the residual brass and Faraday rotation ellipticities and these also account for the asymmetrical appearance of these isolation plots.

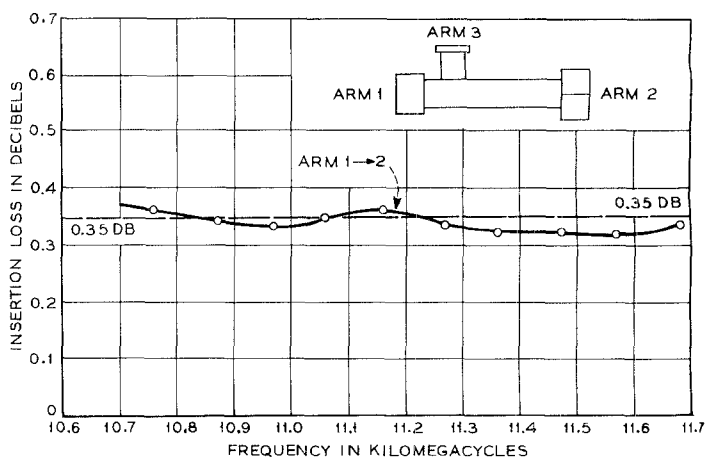


Fig. 23—Circulator insertion loss.

The insertion loss of a typical transmission path is shown in Fig. 23.

V. CONCLUSION

A practical broad-band Faraday rotation circulator can be built and adjusted using a moderate amount of care and a systematic tuning procedure.

Essential characteristics of this general purpose unit for the 10.7-kmc to 11.7-kmc band include a minimum 30-db return loss at each terminal, a minimum isolation of 30 db between nontransmission terminals and a 0.35-db insertion loss between transmission terminals.

The over-all length of this circulator is $16\frac{1}{2}$ inches and it would be difficult to significantly reduce this length below 13 inches without sacrificing bandwidth or some of the isolation characteristics.

The design objectives of this circulator resulted in equal nontransmission path isolations stemming from the ferrite assembly return loss and the Faraday rotation frequency dependence. However, the design emphasis can be readily shifted and in particular the Faraday rotation can be made frequency independent for this bandwidth if one is willing to allow a 0.1-db increase in insertion loss.

